

Article

Strength Analysis in Bonded, Bolted and Bolted-Bonded Joints, Single Lap Joints, Metal/Composite Plates

Ali Sadık and Filiz Karabudak * 

Mechanical Engineering Department, Engineering and Natural Sciences Faculty, Gümüşhane University, 29100 Gümüşhane, Turkey; alisadik1905@gmail.com

* Correspondence: filizkarabudak@gumushane.edu.tr

Abstract: Today, especially in many fields that require structural durability, such as the aerospace and automotive industries, there has been a need to use different bonding techniques separately or together in order to use materials together with different mechanical properties. In this study, stress and damage analysis of single lap joints, bonding and bolt-bonding metal/composite joints under tensile loads were performed. The nine kinds of single lap joint models in different combinations (bonded, bolted and bolt-bonded) were prepared by using acrylic adhesive (Acrytron 1E1) and 100-25-3 mm in size; AZ91/AZ91, AZ91-carbon fiber and carbon fiber-carbon fiber plates. Some comparisons were carried out by examining the stresses and deformations that occur in joint models exposed to tensile and 4-point bending tests. As a result of the tensile test, it was determined that the highest maximum tensile stress occurred in AZ91-CF bolt-bonded samples. In the four-point bending test, the maximum shear force value was determined in the CF-CF bolted-bonded samples.

Keywords: AZ91; bolted-bonding; composite; tensile; bending



Citation: Sadık, A.; Karabudak, F. Strength Analysis in Bonded, Bolted and Bolted-Bonded Joints, Single Lap Joints, Metal/Composite Plates. *Appl. Sci.* **2023**, *13*, 10476. <https://doi.org/10.3390/app131810476>

Academic Editor: Richard (Chunhui) Yang

Received: 19 August 2023

Revised: 8 September 2023

Accepted: 12 September 2023

Published: 19 September 2023



Copyright: © 2023 by the authors. Licensee MDPI, Basel, Switzerland. This article is an open access article distributed under the terms and conditions of the Creative Commons Attribution (CC BY) license (<https://creativecommons.org/licenses/by/4.0/>).

1. Introduction

A bonded joint is a permanent connection formed by connecting two or more parts together with an adhesive layer [1,2]. Metallic adhesives are used to bond two or more metal surfaces strongly and flexibly enough to resist separation, without the need for traditional methods such as nails or screws. These adhesives are natural or synthetic substances [3–6]. Adhesion has made progress with the development of material technology [7]. The use of adhesive in carrier structures, time and cost savings, high corrosion and fatigue resistance, cracking delay, excellent damping properties and other properties has made it an important player in the aerospace and automotive, wood, and plastic industries [8–11]. The usage needs of different materials together has also improved joining techniques and versatility [12]. However, in many applications that require structural durability, combining with adhesive is preferred. Such joints are especially common in the aerospace and automotive industries [13–15].

Adhesive joints have a great impact on making designed systems lighter, stronger, and more economical. Adhesive bonding has more advantages than mechanical bonding [16,17]. These include the ability to combine different thicknesses and types of materials, create joints with equal load distribution, and include the ability to function as a seal [18]. The holes, notches, etc., can also be applied to the surface. It is a cost-effective, simple and fast solution because no joint details or precision machining tolerances are required [19–21]. Despite all these factors, adhesive bonds also have disadvantages. Good adhesion requires proper surface preparation, proper adhesive selection and a suitable environment [8,22]. The strength of such joints is affected by factors such as the surface treatment, material type, adhesive thickness, ambient temperature, and type of load. However, exposure to environmental conditions causes aging over time due to changes in its chemical structure [23]. Due to the properties above, the bond forces and the factors affecting them have been

discussed by many researchers. Adhesive bonding is inexpensive, does not cause crystal structure changes on melting, such as welding, riveting and other types of bonding, does not generate voltage concentrations, and bonds under melting temperatures, resulting in smoother bonding [24–26].

The types of adhesives developed with the use of adhesives have been increasing. In addition, adhesive research continues and people want to benefit from it in every field.

Due to the lightness of magnesium alloys, the specific tensile strength is higher than that of aluminum and steel. Due to the low density of magnesium, it appears to have higher specific strength than aluminum, plastic composite materials, and steels [27–29]. Therefore, magnesium alloys are widely used in the automotive, electronics, defense, and aerospace industries today [30]. In recent years, the use of magnesium alloys in the automotive and aircraft industries has been predicted to increase significantly. Mg-Al-Zn (AZ91) alloy is mostly used for casting automotive and aircraft parts due to its light weight [27,31–33].

AZ91, a magnesium alloy is better at casting properties and better at yielding strength properties than other magnesium alloys. From engines to chassis, the magnesium alloys are used in every part of cars [28,34–36].

In Kelly's 2005 study, he examined using a three-dimensional finite element model that included the effects of load distribution, bolt hole contact, and nonlinear material behavior of the hybrid composite single lap joints. He examined the derail and finite element analysis comparatively and it showed that the hybrid joint showed structurally more advanced performance than adhesive bonding and he produced some harmonious results [37]. Colombi and Poggi used the finite element method in 2006 to eliminate the damage to the adhesive-reinforced gear joint and to ensure this. They investigated in which area the acting force acts on. They showed that one of the two adhesives compared has a fragile structure and the other has a more stable structure. Given these circumstances, it has been concluded that bonding errors can be minimized [38]. In 2011, Reis, et al. compared the shear strength of single lap joint rods from different materials. They combined three different materials. These materials are composite with carbon/epoxy layer, high modulus steel, and 6082-T6 aluminum alloyed materials. The material hardness affects the shear strength, and they stated that the use of the hardest material would provide the highest shear strength. And they showed that the length of the lapping would affect the shear strength which varies according to the material, while the numerical analysis showed that the rotation of the sample decreased with increasing material hardness and resulted in a smoother stress distribution for the six adhesives. They stated that this contributed to the development of shear strength; it was also confirmed by experimental results. They produced high shear strength for steel/steel bonding, but stated that the composite/composite shear strength was lower. They concluded that increasing the hardness of the material would provide a stronger connection [39]. In a 2012 study, Sayman also conducted an analytical elasto-plastic stress analysis used to calculate the shear stress of the single-lap ductile adhesive joint. In this study, the adhesive Dp 460 was used. Sayman used the von Mises criterion to check the flow state of the adhesive. During the analysis, he assumed that the shear stress was constant along the adhesive thickness and ignored the bending moment. The analysis results were confirmed by using finite element analysis. Analytical and numerical results were coherent with each other [40]. In their 2013 study, Liao, et al. experimentally and numerically examined geometric parameters such as overlap length and material thickness for low strength steels (medium and low carbon steels), and material parameters such as adhesive stress–strain. They observed injury patterns in different situations and determined the first place of injury. Unlike the joints made of high-strength steel, they stated that the damage mechanism depended on the leakage of the bonded material. They concluded that the localized tensions at the edges of the winding caused the joining errors in low and medium carbon steels [41]. In 2014, Rahman and Sun determined an accurate damage prediction criterion usable to predict the stress of tear damage to fibers by using a field-based approach. They experimentally determined the type of damage by using carbon fiber composites, epoxy adhesive and splices of various sizes. They tested

several voltage/strain-based failure criteria for composites. They calculated the size of the critical fields with the help of finite element analysis by using the known collapse loads of single lap joints. As a result, they found that the Azzi–Tsai criterion (Norris) was appropriate for estimating the stress of fiber tear damage in single rots [42]. In a paper in 2018, Selahi made an error analysis on an ANSYS Workbench by applying shear and bending loads to double lap joints with hybrid bonded and single bolted laminated composite adhesions exposed to axial effects by using three-dimensional finite element simulation. Simulation analysis was compared with literature studies. It was concluded that there was a significant increase in bonded joints at the rate of 56% when compared to bonded joints [43]. In their study in 2014, Silva and Nunes tested nine aluminum-epoxy single lap joint samples with different adhesive thicknesses and outer bonded segment ratios under tensile loading. They estimated the deviations of single lap joint samples by using the digital image correlation method. They also examined the Hart-Smith, Goland and Reissner models and modified the Goland and Reissner models to compare the theoretical prediction by using experimental data. Improvement in the Goland and Reissner model proposed by Tsai-Morton was examined. The improvement in the Goland and Reissner model proposed by Tsai-Morton concluded that the single lap joints studied would be more appropriate to explain their mechanical behavior. As a result, they determined that the proposed alternative methodology would be a good way to predict the moment of bending [44]. In their study, Li et al. (2020) conducted an experimental examination of the tensile property of single-lap joints in carbon-fiber-reinforced bismaleimide (BMI) resin composite laminates. The effect on the tensile feature of single lap joints of the stacking order and width/diameter ratio of composite laminates with three joint configurations, which are bolted, bonded with adhesive and hybrid bolted/bonded single lap joints, was discussed. They concluded that the stacking order and W/D ratio are important in the design of the joints, and the bolts in hybrid joints can increase the tensile property after adhesive failure [45]. In their study, Ye et al. (2018) conducted a comprehensive study of the composite single-lap joints with adhesive-resistant strength. They created 3D open models of single-lap joints with different overlap lengths which were subjected to uniaxial tensile load. They compared the efficiency and accuracy of the models, load-displacement curves, and damage morphology with numerical and experimental results. They concluded that the load displacement curves were consistent with the experimental results and that the fault morphology could be predicted according to the model types [46]. In their study, Belardi et al. (2021) examined the capabilities of the single lap multi-bolted composite joints and composite bolted joint elements (CBJEs). In particular, it was shown that a simplified FE model, which includes shell elements to simulate plates and CBJEs for the bolted zone, can reliably determine the bolt load distribution and secondary bending of the joint. They compared experimental data of single lap three-bolted composite joints with FE theoretical data. They concluded that the obtained data could be used profitably for the design of the joint [47]. In their study, Chen et al. (2019) investigated both the mechanical behavior and damage mechanism of riveted, joined and hybrid carbon fiber-reinforced plastic (CFRP)-aluminum joints with various overlap lengths. They analyzed the load-displacement curves, peak load, energy absorption, and joint stiffness. They used high-resolution micrographs of the broken surface to understand various failure modes in the CFRP-aluminum composite by taking typical failure development photos with a high-speed camera for progressive failure analysis. According to the experimental results, they showed that hybrid joints offer superior performance in terms of peak load and energy absorption, increasing up to ~380%, 434% and ~19%, 56%, respectively, only when compared to riveted and joined joints [48].

In the light of the literature studies, in this study bonded, bolted and bolted-bonded single lap joint elements were mechanically analyzed under the static tensile and bending loads. Acrytron 1E1, a high-performance, acrylic-based metal adhesive, was preferred as an adhesive. In recent years, AZ91 magnesium alloy and carbon fiber plate materials used in the aerospace and automotive industries due to their mechanical properties such as

high specific strength and light weight have been deployed as bonding surfaces [49]. This study is unique because the bonded, bolted and bolted bonded single lap joint made with Acryton 1E1 adhesive, which is especially an AZ91 plate material and an Acrylic adhesive type used in the study, is not found in any other study.

2. Materials and Methods

In this study; bonded, bolted and bolted-bonded single-lap joints were formed with AZ91 Mg alloy (the chemical composition in Table 1) and carbon fiber composite plates (100-25-3 mm) by using Acrylic Acrytron 1E1 adhesive. Lap joints were made using the ASTM D3165-07 standard [50]. The plates used for tensile tests and manufactured according to the ASTM 3039 standard [51]. Four-point bending test samples were manufactured according to the ASTM D 1002 standard [52]. Tensile and four-point bending tests were performed to determine the mechanical properties of AZ91 and the carbon fiber plates, which form single-lap bonded, bolted and bolted-bonding joints. The metallographic structure of the adhesive that broke after mechanical tests was examined with the help of an optical microscope. In the test, six samples from each panel were tested and the stress and damage analysis values were compared and evaluated. The geometric dimensions of all lap joints are shown in Figures 1–3.

Table 1. Chemical composition of alloy AZ91 Mg [53].

AZ91	Al	Zn	Mn	Si	Cu	Mg
%	8.84	0.61	0.18	0.02	0.005	Balance

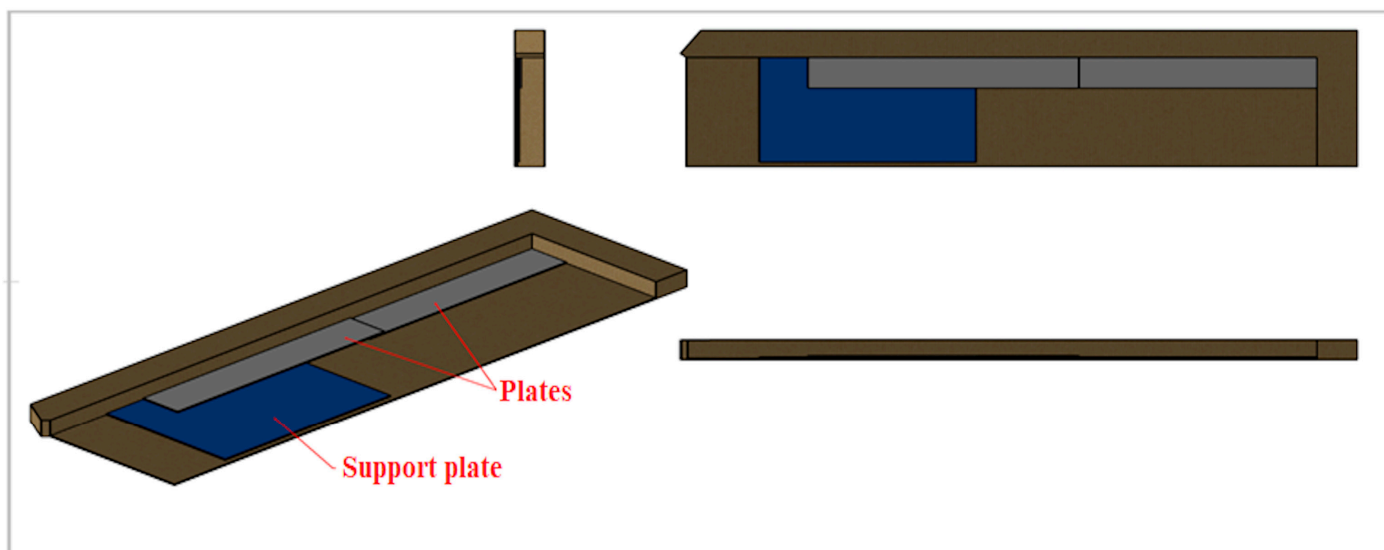


Figure 1. Schematic mold image used for production in single lap bonding joints.

AZ91 Mg alloy has mechanical values as a 65.3 HV stiffness, a 212.6 MPa tensile strength, a 120.5 MPa 0.2% yield strength and a 4.8% elongation [54]. Carbon fiber composite plates with a density of 1.8 g/cm³ have mechanical properties such as a 2.1% elongation at break, 4a 900 MPa tensile strength and a 230 GPa tensile modulus [55].

Method

The mold was used to adjust the lap length and adhesive thickness to optimum dimensions, to keep the bonded materials stable in their current position during the adhesion process, and to prevent the material from flowing to the edges while the adhesive was hardening (Figures 1–3). The material surfaces to be bonded before bonding were roughened to provide a cohesive bond. During the bonding process, the adhesive was applied to the adhesion surfaces with a special gun, and the adhesive was distributed in

the adhesive area properly and was exposed to equal pressure in order to apply a certain adhesion pressure. The adhesives were kept at room temperature for a 24-h curing time and made ready for tests. Nine separate joint groups were formed to bond in the forms of AZ91-AZ91, AZ91-carbon fiber and carbon fiber-carbon fiber materials, bolted and bolt-bonded. Six tensile and four-point bending test samples were prepared according to the standards from each of the single lap plate groups.

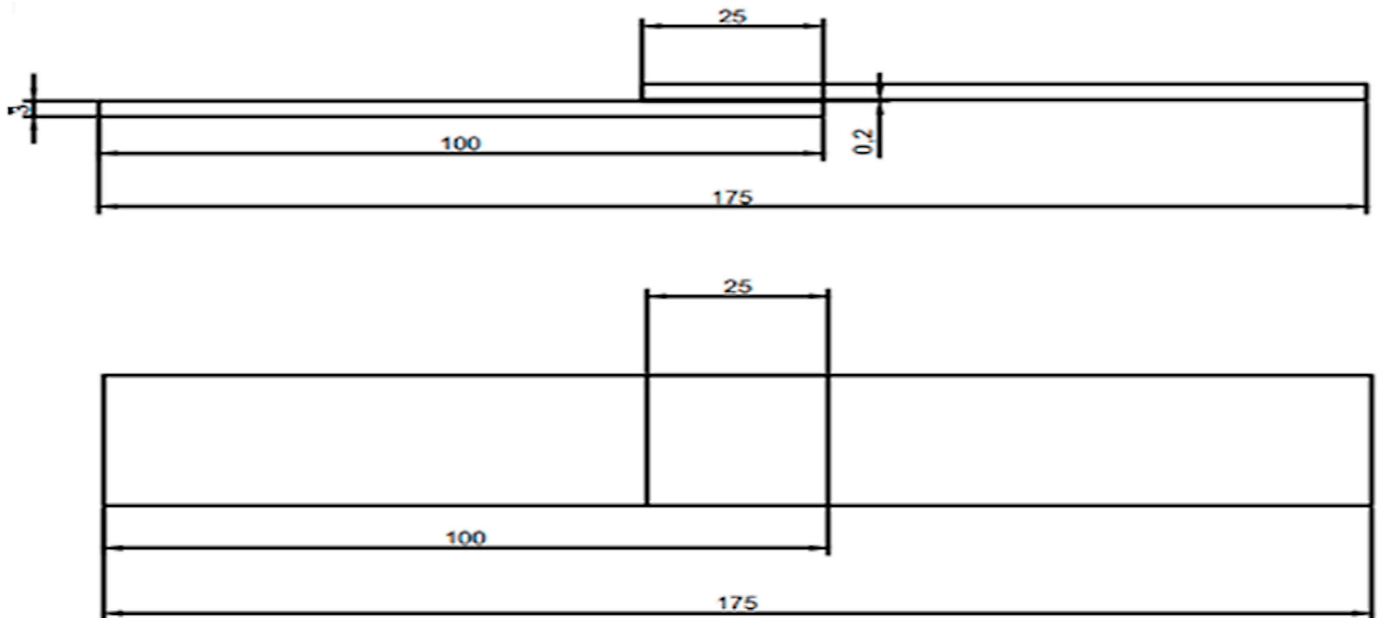


Figure 2. Measures of single lap bonding joints (measures mm).

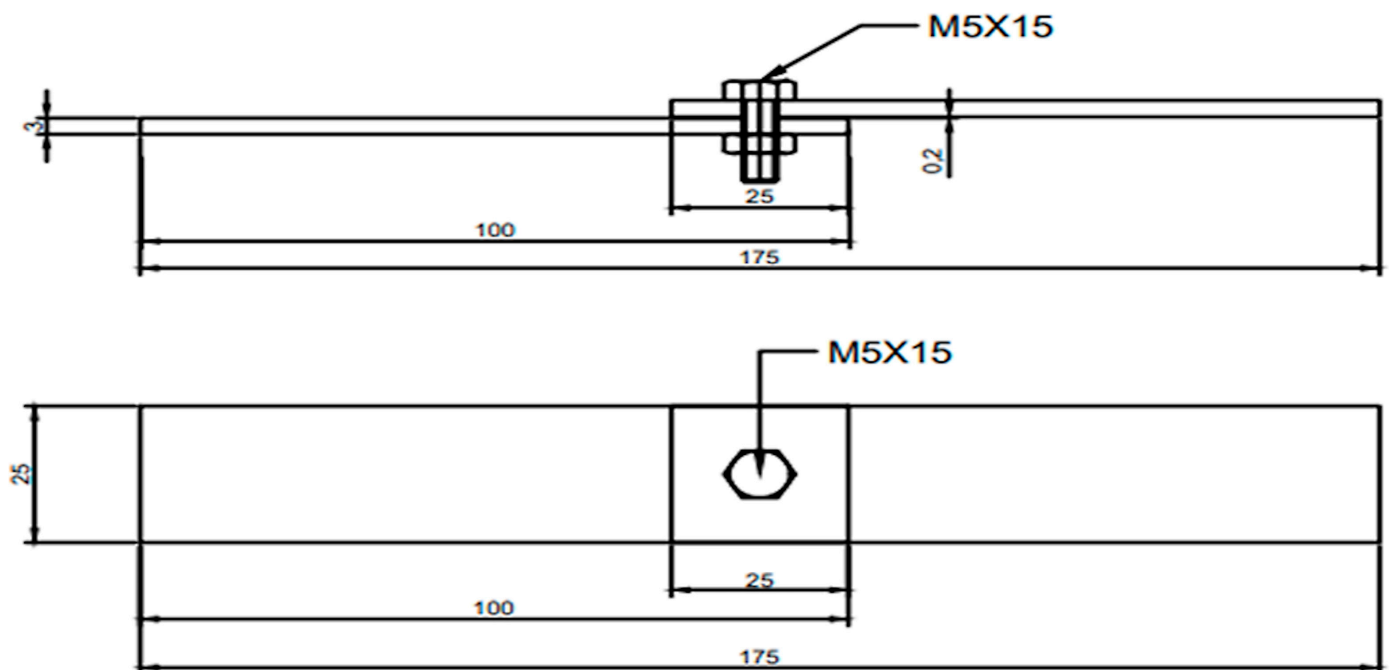


Figure 3. Measure of single lap bolted and bolted-bonding (measures mm).

The manufacturing process of samples manufactured according to the dimensions specified by ASTM D3165-07 is similar to the TAST type (ASTM D3165-07, 2014). No fixtures were used to connect. After the short and long edges of the parts to be assembled

were supported by a forehead, production was performed by placing another plate of the same thickness from the ground under the parts (Figure 1).

Figure 4 shows the schematic damage view of the samples after the four-point bending test.

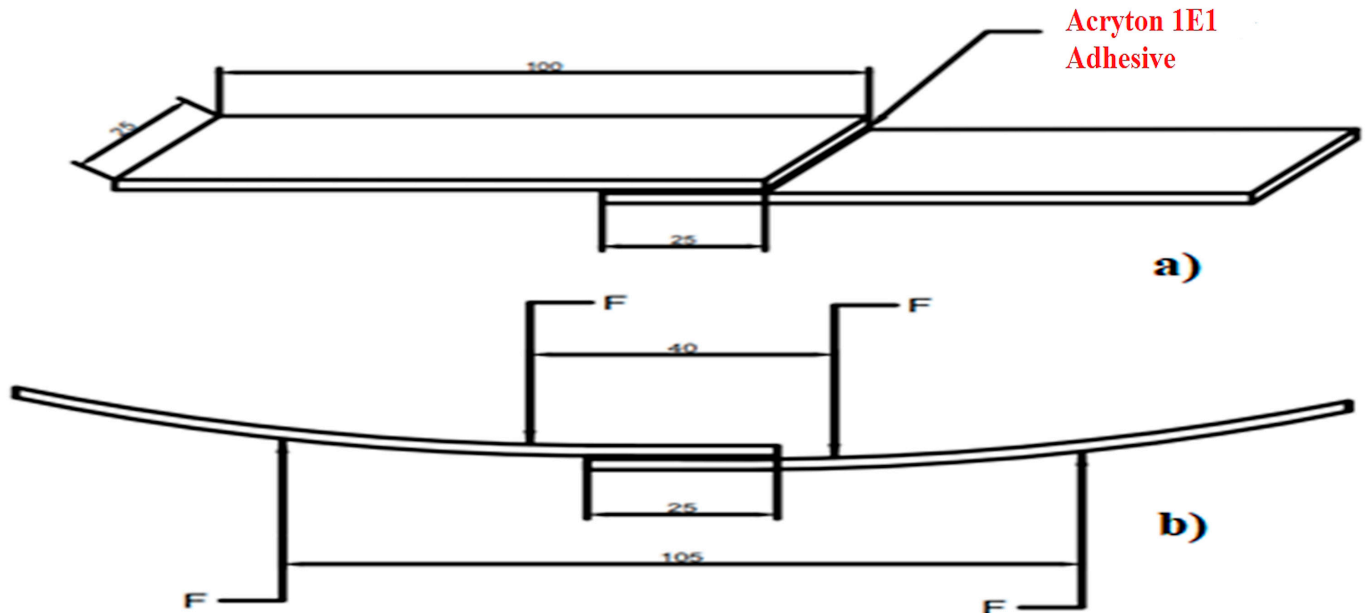


Figure 4. Sample of four-point bending test (a) measures (b) schematic image after damage.

The tensile test of single lap bonding joints was performed in the BESMAK BMT 200ES model, universal axial tensile tester with a capacity of 20 KN, at room temperature and at 1 mm/min tensile speed. Bending tests were performed at room temperature and 2 mm/min bending speed by using the Instron universal test machine. All tensile and four-point bending tests were performed in six repetitions (Figure 5).

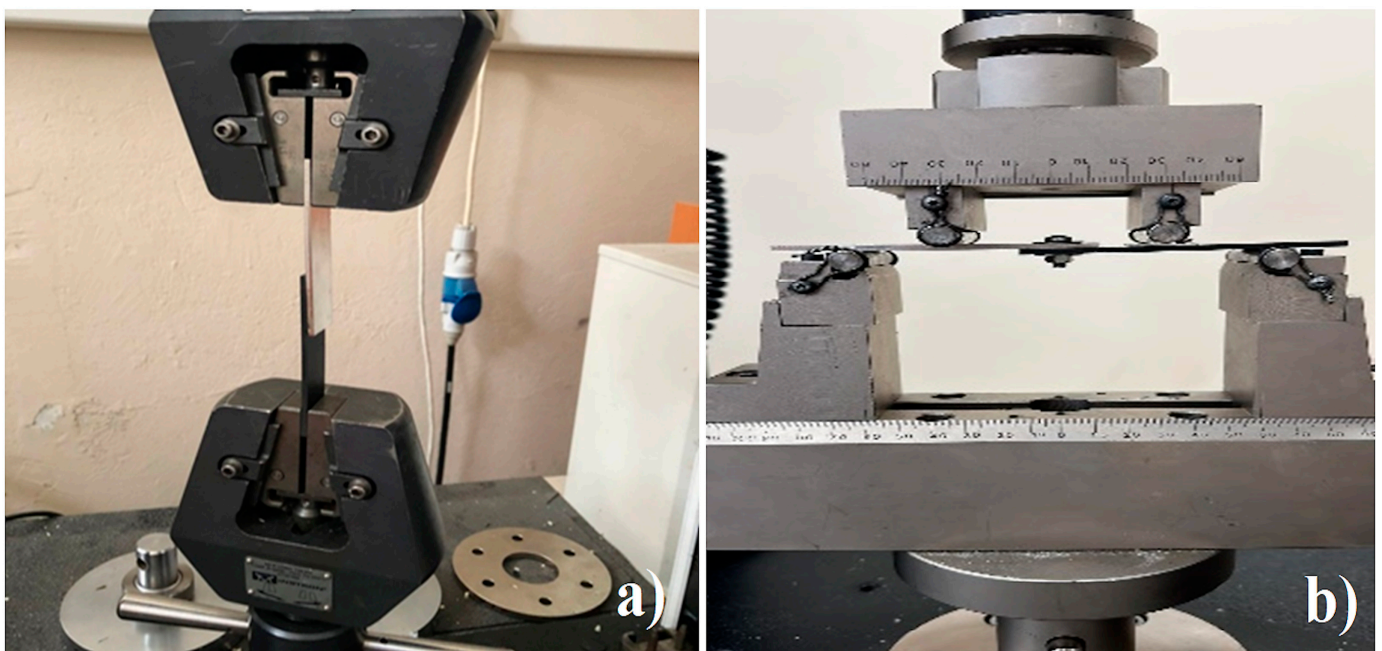


Figure 5. Tester (a) Tensile (b) Bending.

In Table 2, the test types applied to all joints models and the obtained values as a result of the analysis are summarized.

Table 2. All joint points were performed and tested in the study (T = tensile test B = four-point bending test).

	AZ91-AZ91-Bonded	AZ91-AZ91-Bolted	AZ91-AZ91-Bolted-Bonded	CF-CF-Bonded	CF-CF-Bolted	CF-CF-Bolted-Bonded	AZ91-CF-Bonded	AZ91-CF-Bolted	AZ91-CF-Bolted-Bonded
Maximum Stress (MPa)	T	T	T	T	T	T	T	T	T
Maximum Force (N)	T/B	T/B	T/B	T/B	T/B	T/B	T/B	T/B	T/B
Maximum Elongation (%)	T	T	T	T	T	T	T	T	T
Maximum Elongation (mm)	T	T	T	T	T	T	T	T	T
Damage Type	T/B	T/B	T/B	T/B	T/B	T/B	T/B	T/B	T/B
Displacement (mm)	B	B	B	B	B	B	B	B	B
Standard Deviation	T/B	T/B	T/B	T/B	T/B	T/B	T/B	T/B	T/B

3. Research Findings and Discussion

3.1. Tensile Test Results

3.1.1. AZ91-AZ91; Bonded, Bolted and Bolted-Bonded Single Lap Plates

In this section, there are the results obtained from experimental studies of AZ91-AZ91 single lap plates, which are arranged with geometric parameters bonding, bolted and bolted-bonded.

As shown in Figure 6d and Table 3, according to the tensile test results, the maximum tensile stress (max shear) is 34.68 MPa, the maximum tensile elongation is 2.93 mm, the maximum tensile force is 5202.26 N, and the maximum tensile elongation is 11.74 mm value. In Figure 6a, partial breaks seen in the adhesive on both surfaces in bonded samples indicate that the adhesive has good adhesion. In bolted samples (Figure 6b), a crush occurred in the hole in the lower and upper part. The bolt, on the other hand, has breaking damage. In the upper and lower part, where partial ruptures occur in bolted-bonded samples (Figure 6c), it can be seen that the adhesive on the plate has good adhesion. While crushing occurred in the holes in the lower and upper parts, fracture damage occurred in the bolt.



Figure 6. Cont.

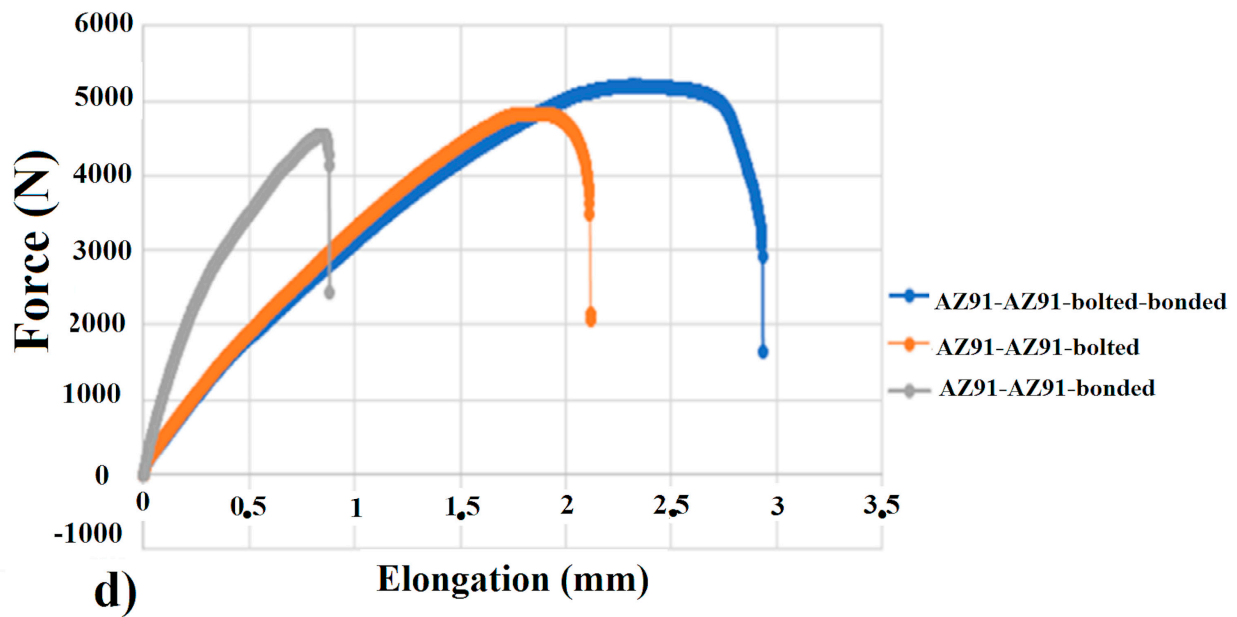


Figure 6. AZ91-AZ91 (a) bonded, (b) bolted (c) bolted-bonded single lap plate-linked samples tensile test damage image after tensile test and (d) force-elongation diagram.

Table 3. Damage type, standard deviation and tensile test values of AZ91-AZ91 bonded, bolted and bolted-bonded single lap plate joints.

	Maximum Tensile Stress (MPa)	Maximum Tensile Force (N)	Maximum Tensile Elongation (%)	Maximum Tensile Elongation (mm)	Damage Type	Standard Deviation
AZ91-AZ91-bonded	30.31	4547.25	3.52	0.88	Local rupture in adhesive	1.40
AZ91-AZ91-bolted	32.19	4829.14	8.46	2.11	Crushing in the hole, breaking in the bolt	1.22
AZ91-AZ91-bolted-bonded	34.68	5202.26	11.74	2.93	Crushing in the hole, breaking in the bolt, local rupture in adhesive	1.10

3.1.2. Carbon Fiber-Carbon Fiber; Bonded, Bolted and Bolted-Bonded Single Lap Plates

In this section are results obtained from the experimental studies of Carbon Fiber-Carbon Fiber single lap plates, which are arranged with geometric parameters bonding, bolted and bolted-bonded.

As seen in Figure 7d and Table 4, according to the tensile test results, bolted-bonded samples are seen that the value is 5677.25 N in the maximum tensile force and is 3.11 mm in tensile elongation. In Figure 7a, it can be seen that the adhesive on the plate in the upper and lower part has good adhesion. Partial breaks occurred as a result of the tensile elongation. In bolted samples (Figure 7b), a crush occurred in the hole in the lower and upper part. Breaking damage occurred in the bolt. It can be seen that the adhesive has good adhesion on the upper and lower plate, where partial ruptures occur as a result of the tensile test in bolted-bonded samples (Figure 7c). When there was crushing in the holes in the lower and upper parts, fracture damage occurred in the bolt.

3.1.3. AZ91-Carbon Fiber; Bonded, Bolted and Bolted-Bonded Single Lap Plates

As shown in Figure 8d and Table 5, according to the tensile test results, it can be seen that the maximum pulling force is 5786.65 N and the tensile elongation is 3.05 mm in bolted-bonded samples. According to Figure 8a, it can be seen that the adhesive has good adhesion in the upper and lower plate in the samples with adhesive single lap plate joints. Partial breaks occurred as a result of the tensile elongation. In bolted samples (Figure 8b), crushing occurred in the holes in the lower and upper part, while fracture damage occurred in the bolt. In bolted-bonded (Figure 8c) samples, it can be seen that the adhesive on the

plate in the upper and lower parts has good adhesion. While crushing occurred in the holes in the lower and upper parts, fracture damage occurred in the bolt.

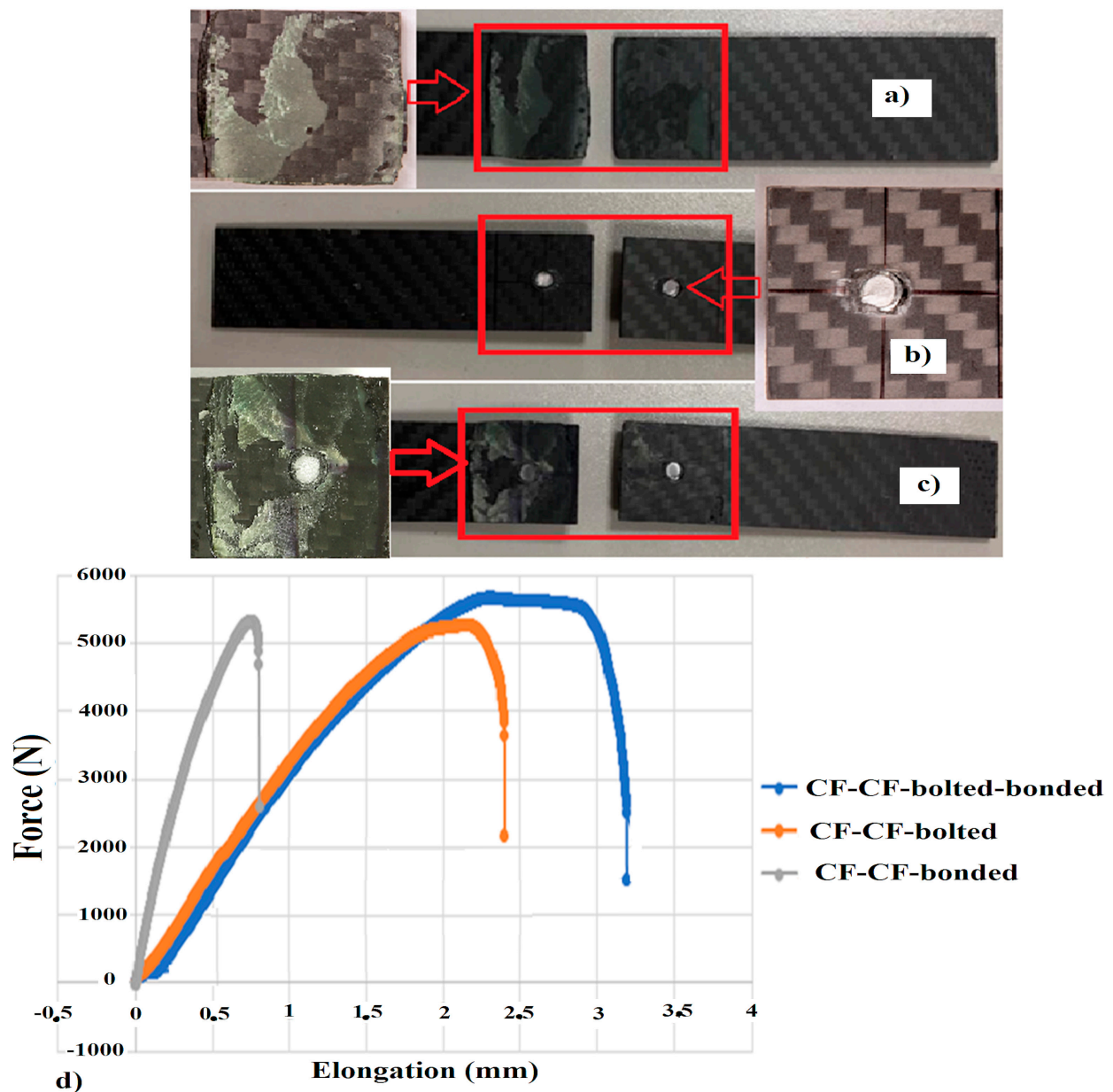


Figure 7. Damage image after tensile test of CF-CF (a) bonded, (b) bolted (c) bolted-bonded single-lap plate-linked samples and (d) force-elongation diagram.

Table 4. Damage type, standard deviation and tensile test values of CF-CF bonded, bolted and bolted-bonded single lap plate joints.

	Maximum Tensile Stress (MPa)	Maximum Tensile Force (N)	Maximum Tensile Elongation (%)	Maximum Tensile Elongation (mm)	Damage Type	Standard Deviation
CF-CF-bonded	34.49	5323.75	3.21	0.80	Local rupture in adhesive	1.34
CF-CF-bolted	35.11	5266.73	9.58	2.39	Crushing in the hole, breaking in the bolt	1.12
CF-CF-bolted-bonded	37.84	5677.25	12.76	3.19	Crushing in the hole, breaking in the bolt, local rupture in adhesive	1.07

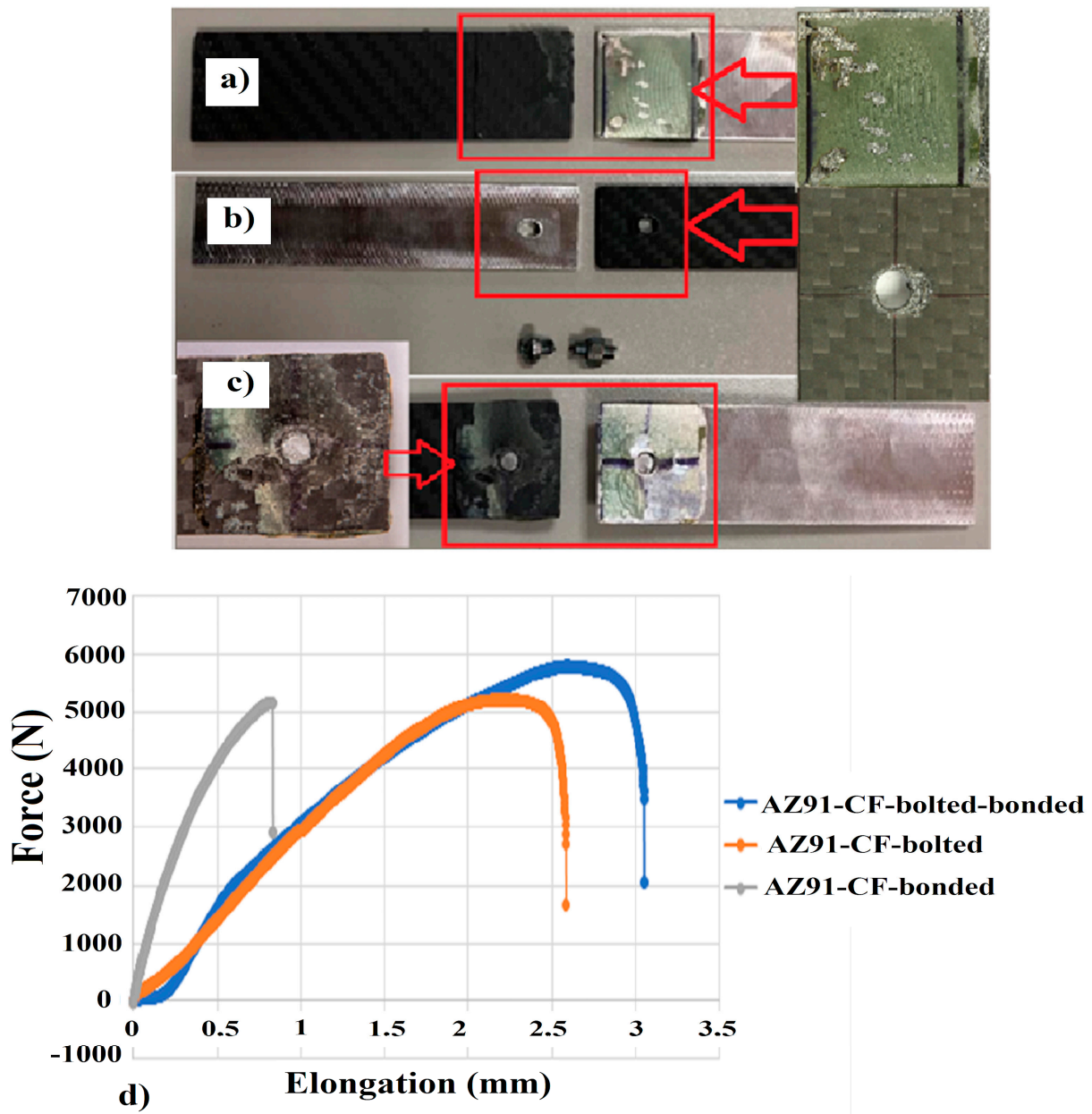


Figure 8. AZ91-CF (a) bonded, (b) bolted (c) bolted-bonded- single-lap plate-connected samples damage image after tensile test and (d) force-elongation diagram.

Table 5. Damage type, standard deviation and tensile test values of AZ91-CF bonded, bolted, and bolted- bonded single lap plate joints.

	Maximum Tensile Stress (MPa)	Maximum Tensile Force (N)	Maximum Tensile Elongation (%)	Maximum Tensile Elongation (mm)	Damage Type	Standard Deviation
AZ91-CF-bonded	34.41	5162.25	3.33	0.83	Local rupture in adhesive	1.23
AZ91-CF-bolted	34.69	5203.81	10.33	2.58	AZ91 Crushing in the hole, Delamination Breaking in the bolt	1.08
AZ91-CF-bolted-bonded	38.57	5786.65	12.20	3.05	AZ91 Crushing in the hole, breaking in the bolt, local rupture in adhesive	1.03

3.1.4. AZ91-AZ91, AZ91-Carbon Fiber and Carbon Fiber-Carbon Fiber; Bonded, Bolted and Bolted-Bonded Single Lap Plates

When Figure 9 and Table 6 are examined, in Figure 9a it can be seen that the maximum tensile force is 5323.75 N and the tensile elongation in AZ91-AZ91 plates is 0.80 mm in the CF-CF bonded samples plate. In Figure 9b, it can be seen that the maximum tensile force is 5266.73 N in CF-CF bonded plates and the tensile elongation is 2.58 mm in the AZ91-CF bonded plate. In Figure 9c, it can also be seen that the maximum tensile force is 5786.65 N in CF-CF bonded plates and the tensile elongation is 3.19 mm in bolted adhesive samples.

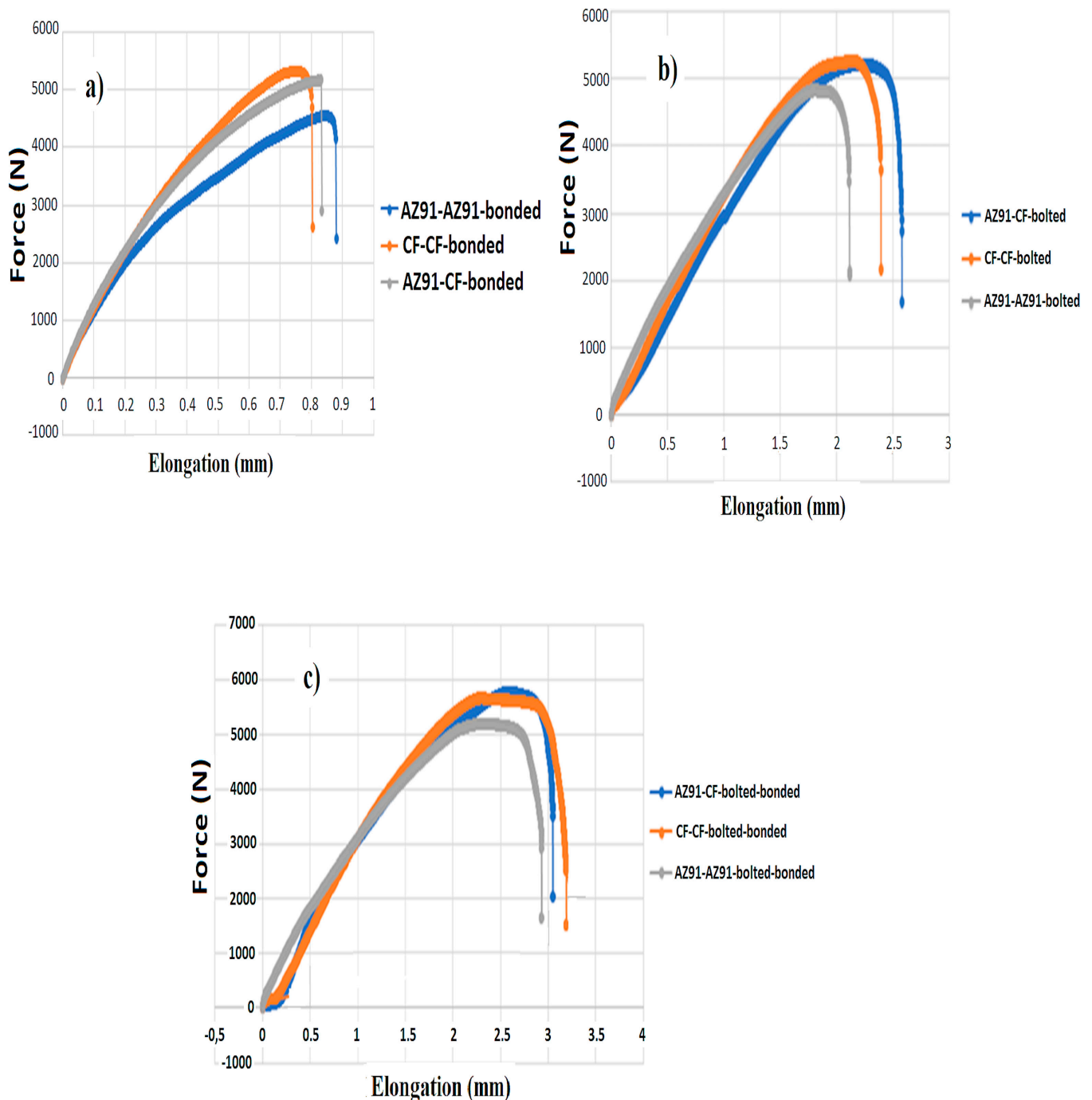


Figure 9. Force-elongation diagram of AZ91-AZ91, AZ91-Carbon fiber and carbon fiber-carbon fiber (a) bonded (b) bolted and (c) bolted-bonded single lap plate joints.

Table 6. AZ91-AZ91, AZ91-carbon-fiber and carbon fiber-carbon fiber; tensile test values of bonded, bolted and bolted-bonded single lap plate joints.

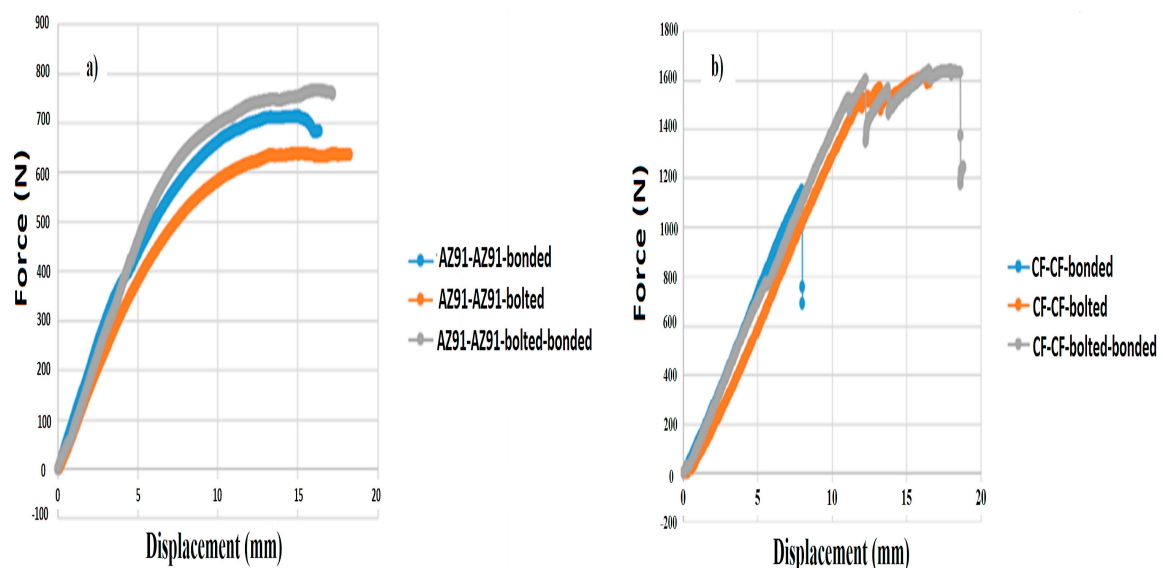
	Maximum Tensile Stress (MPa)	Maximum Tensile Force (N)	Maximum Tensile Elongation (%)	Maximum Tensile Elongation (mm)
AZ91-AZ91-bonded	30.31	4547.25	3.52	0.88
AZ91-AZ91-bolted	32.19	4829.14	8.46	2.11
AZ91-AZ91-bolted-bonded	34.68	5202.26	11.74	2.93
CF-CF-bonded	34.49	5323.75	3.21	0.80
CF-CF-bolted	35.11	5266.73	9.58	2.39
CF-CF-bolted-bonded	37.84	5677.25	12.76	3.19
AZ91-CF-bonded	34.41	5162.25	3.33	0.83
AZ91-CF-bolted	34.69	5203.81	10.33	2.58
AZ91-CF-bolted-bonded	38.57	5786.65	12.20	3.05

In line with these data, it was determined that maximum tensile stress and maximum tensile elongation were seen in bolted- bonded samples, and the highest tensile stress value occurred in AZ91-CF bolted- bonded samples while the maximum elongation value occurred in CF-CF bolted- bonded samples. When considering the tensile force and elongation of the adhesive joints under tensile test, it can be seen that it receives values in the bonded < bolted < bolted- bonded order.

No peeling effect or plastic deformation was observed on the bonded surfaces. Plastic deformation was observed in bolted and bolted bonded samples and delamination damage was observed in the holes in the carbon fiber materials. It can be seen that bolt holes are deformed along the loading direction in all samples and fiber extraction and delamination occur around the hole in carbon fiber samples.

3.2. Four Point Bending Test

In Figure 10a, the maximum shear force (~780 N) is seen in AZ91-AZ91bolted-bonded samples and maximum displacement (~18 mm) in bolted samples. In displacement bolted-bonded samples, it has also a high value ratio of 17 mm. In Figure 10b, the maximum shear force (~1600 N) can be seen in CF-CF-bolted-bonded CF-CF-bolted samples, and the maximum displacement (~17 mm) can be seen in the same samples. In Figure 10c, the maximum shear force (~850 N) can be seen in AZ91-CF-bonded samples and the the maximum displacement (~17 mm) is in AZ91-CF-bolted-bonded samples.

**Figure 10.** Cont.

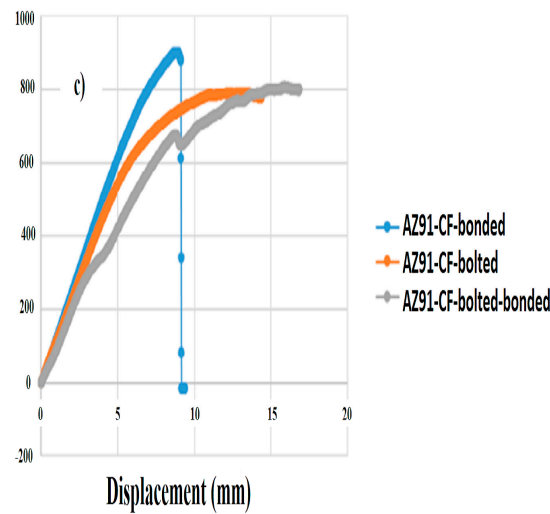


Figure 10. (a) AZ91-AZ91, (b) Carbon fiber-Carbon fiber and (c) AZ91- Four-point bending test force-displacement graph of carbon fiber bonded, bolted and bolted-bonded single lap plate joints.

In Figure 11a, the maximum shear force can be seen in CF-CF-bonded samples with ~1200 N and the maximum displacement in samples AZ91-AZ91 is ~16 mm. In Figure 11b, the maximum shear force can be seen in CF-CF-bolted samples with ~1600 N and the maximum displacement is in AZ91-AZ91-bolted samples with ~18 mm. In Figure 11c, it can also be seen that the maximum shear force is in CF-CF-bolted-bonded samples with ~1600 N and the maximum displacement is in CF-CF-bolted-bonded samples with ~18 mm.

When the damage images as a result of the four-point bending test are examined in Figure 12, it can be seen that CF-CF bonded samples in Figure 12d and AZ91-CF bonded samples in Figure 12g the plates are separated from each other because the adhesive is broken, but in Figure 12a AZ91-AZ91 bonded samples did not break but they only bent like other bolted and bolted-bonded samples. This shows that bonded samples cannot carry the load and break. It can also be concluded that the adhesive has better adhesion in AZ91 samples than carbon fiber samples. The absence of peeling in the separated samples (Figure 12d,g) indicates that there is good adhesion at the adhesive and material interface. Table 7 shows the standard deviation values of single lap plate joints.

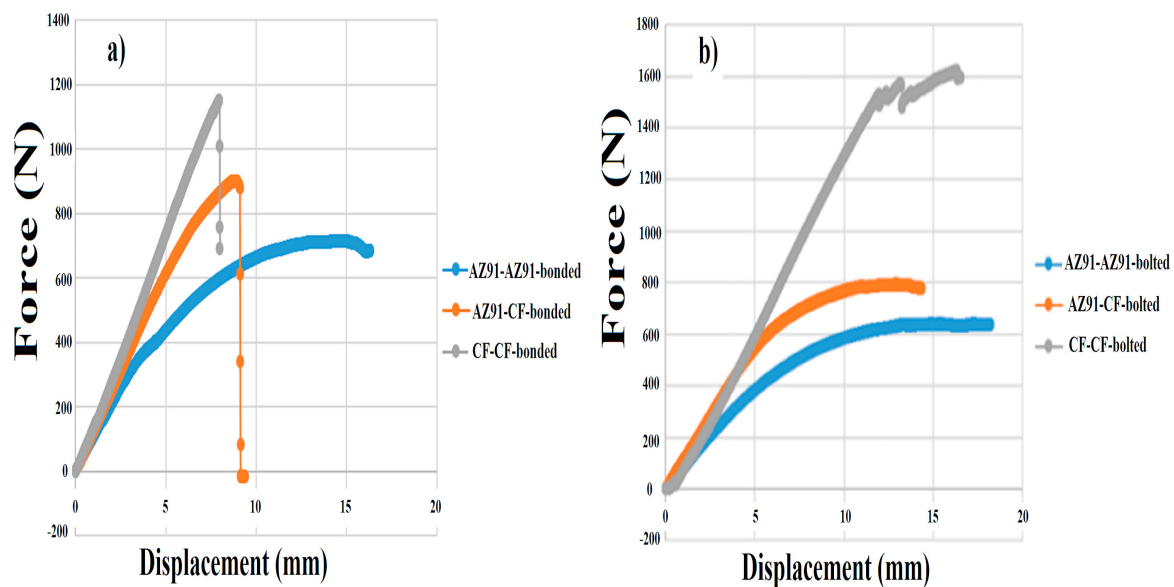


Figure 11. Cont.

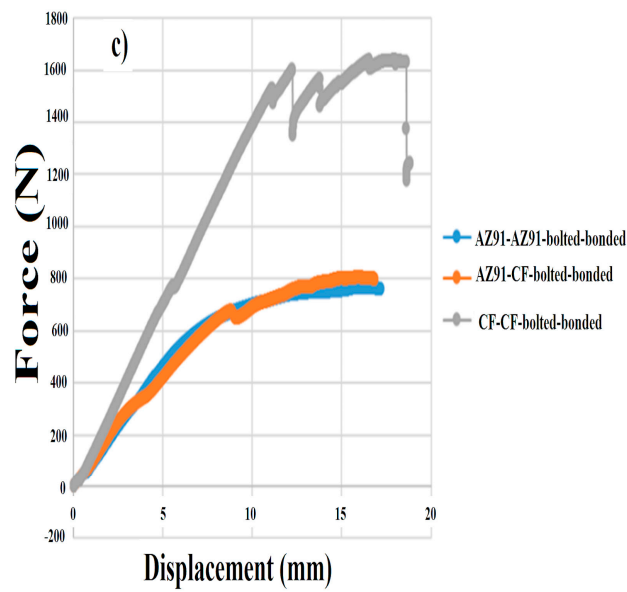


Figure 11. AZ91-AZ91, AZ91-carbon-fiber and carbon fiber-carbon fiber single-lap plate joints (a) bonded, (b) bolted and (c) bolted- bonded four-point bending test force-elongation graph.

Table 7. Bending test standard deviation values of AZ91-AZ91-carbon-fiber and carbon fiber-carbon fiber bonded, bolted and bolted- bonded single lap plate joints.

AZ91-AZ91-Bonded	AZ91-AZ91-Bolted	AZ91-AZ91-Bolted-Bonded	CF-CF-Bonded	CF-CF-Bolted	CF-CF-Bolted-Bonded	AZ91-CF-Bonded	AZ91-CF-Bolted	AZ91-CF-Bolted-Bonded
1.60	1.42	1.38	1.55	1.22	0.97	1.29	0.99	0.67

When the four-point bending tests of AZ91-AZ91, AZ91-CF, CF-CF-CF bonded, bolted and bolted- bonded single lap plate joints are evaluated together in Figure 13, it can be seen that the maximum shear force is ~1600 N in CF-CF-bolted-bonded samples and the maximum displacement is ~18 mm in CF-CF-bolted-bonded.

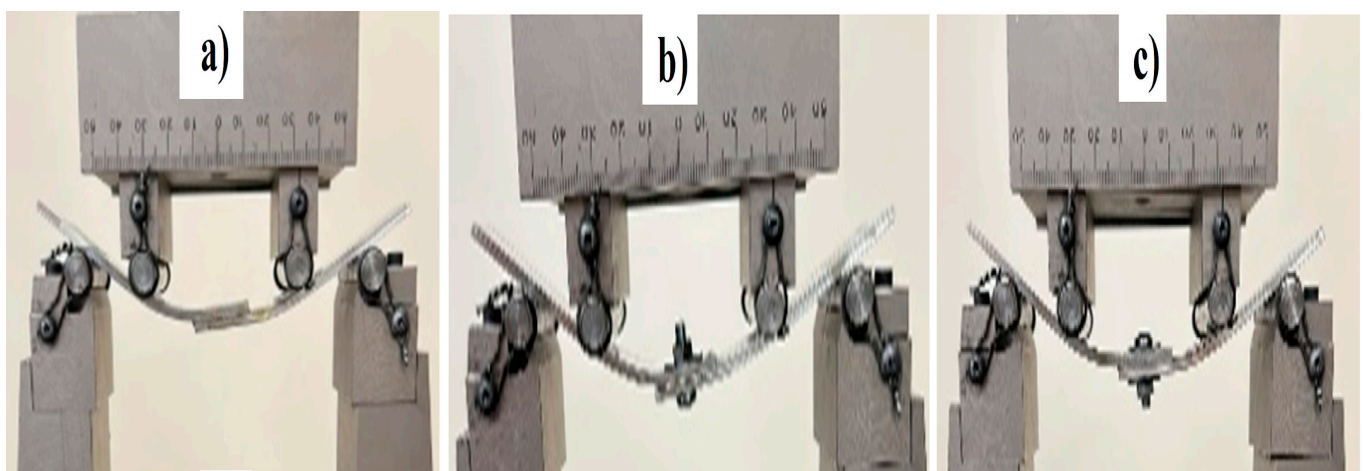


Figure 12. Cont.

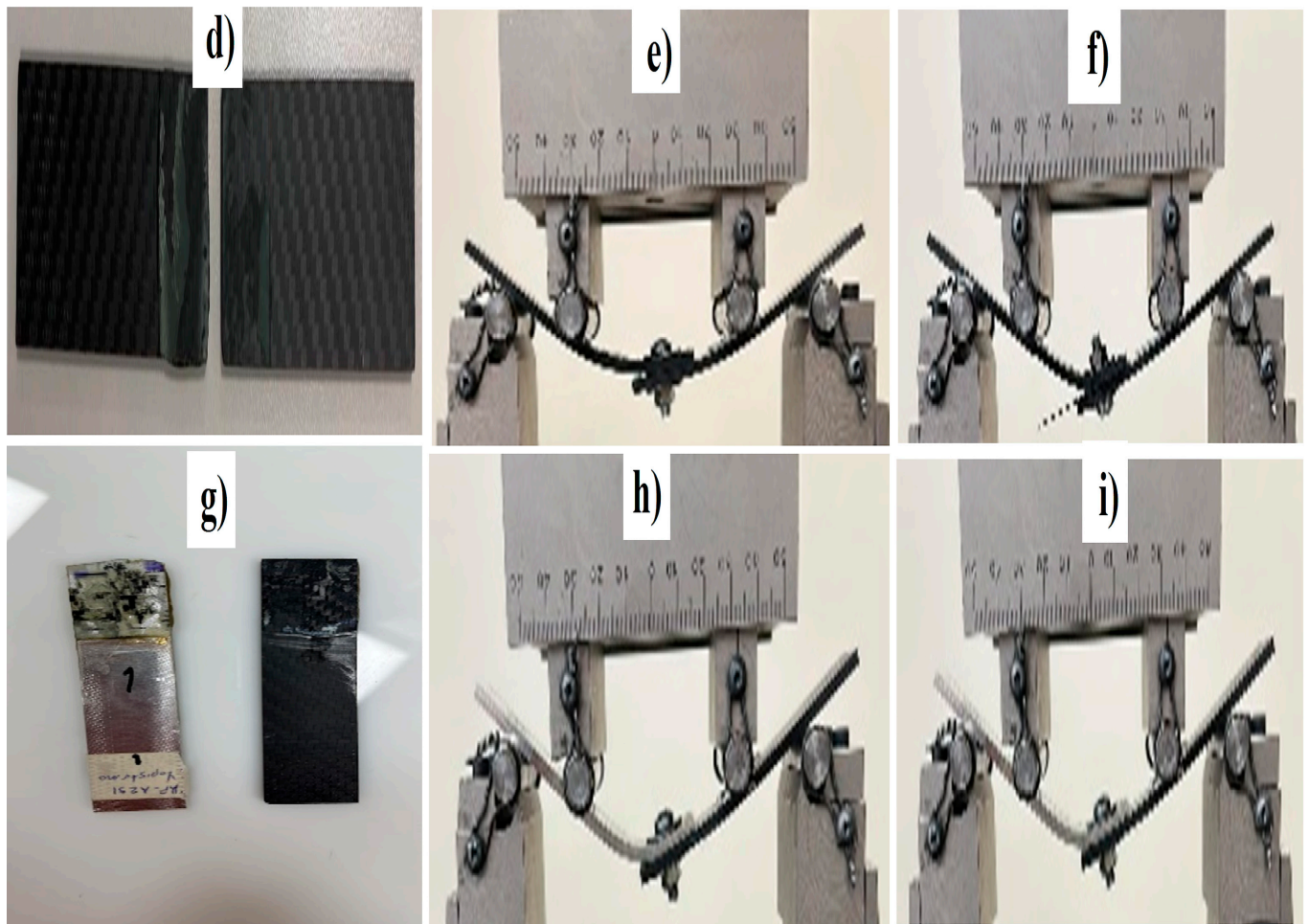


Figure 12. AZ91-AZ91; (a) bonded, (b) bolted and (c) bolted-bonded, CF-CF; (d) bonded, (e) bolted and (f) bolted-bonded, AZ91-CF, (g) glued, (h) bolted and (i) bolted-bonded single lap plate joints.

Various studies have been carried out to increase the mechanical properties of the AZ91 alloy. Aging after homogenization is one of the known processes of increasing its mechanical properties. In the first studies, it was shown that the resistance also increased as its sediment increased. As is known, the AZ91 Mg alloy contains the β -Mg₁₇Al₁₂ precipitate phase in addition to the α -Mg phase, which is the matrix phase. In their study, Motavallian et al. (2023) investigated the effects on the structural, mechanical, and bio corrosion properties of a solid-soluted AZ91 alloy by adding bioactive glass (BG) to the AZ91 alloy with the friction-stir backward extrusion method (FSBE). They concluded that the formation of a discontinuous β -Mg₁₇Al₁₂ phase within the α -Mg matrix and the presence of bioactive glass particles would contribute to higher corrosion resistance of the AZ91-bioactive glass composite wire [56]. In addition, many researchers have investigated physical and chemical modification methods for better charge transfer from mineral matrices to CFs. In addition to adapting the interphase region between polymer impregnations and temperature-resistant mineral suspensions, CF wicks, and surrounding matrices, surface modification approaches such as oxidation, electrophoretic deposition, plasma, and inoculation treatments have also been applied to improve fiber-matrix interactions [57]. In their carbon fiber modification study (2023), Lu et al. proposed a long fiber modification method in which carbon fiber filaments were first modified and then easily dispersed by dividing them into short fibers, and modified carbon fiber reinforced cemented composites could have good properties [58]. It is predicted that the improved AZ91 and its carbon fiber microstructure may be effective in adhesive material and material

interface, adhesion and strength in the single-lap joint types obtained by bonding the AZ91 Mg alloy and the carbon fiber composite plate with adhesive.

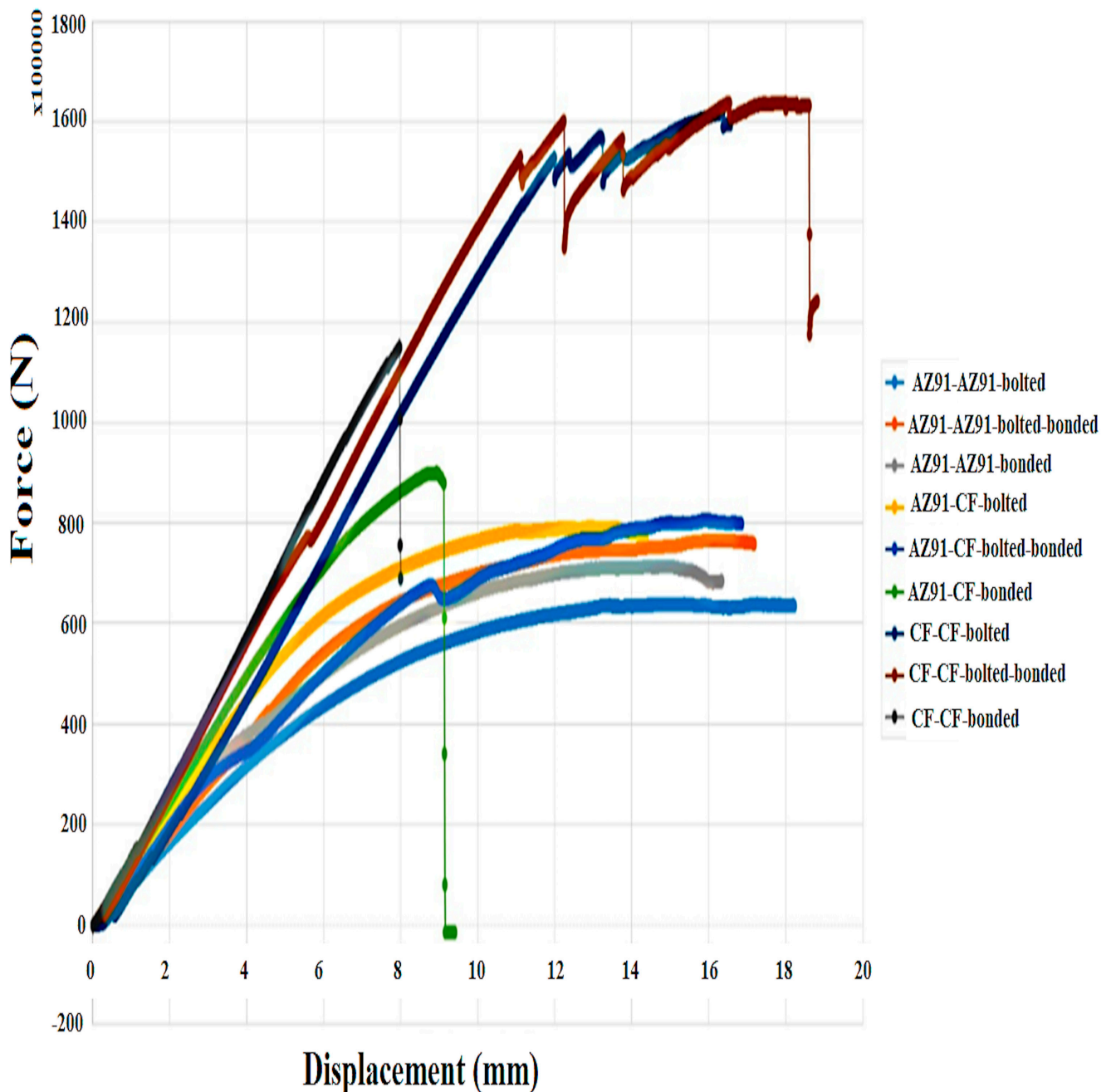


Figure 13. AZ91-AZ91, 4 point bending test force (f)-displacement (mm) graph of AZ91-fiber and carbon fiber-carbon fiber bonded, bolted and bolted- bonded single lap plate joints.

4. Conclusions

In this study, the following analysis results were concluded with tensile and four-point bending tests by creating nine separate single lap joints groups and by bonding AZ91-AZ91, AZ91-carbon fiber and carbon fiber-carbon fiber materials bonded, bolted and bolted-bonded forms:

- According to force–elongation values obtained from the tensile test of AZ91-AZ91, AZ91-CF, CF-CF bonded, bolted and bolted-bonded single lap plate joints, the highest maximum tensile stress was determined in AZ91-CF bolted-bonded samples and the highest maximum tensile elongation occurred in CF-CF bolted-bonded samples. Ten-

sile force and elongation of the bonding joints receive values in the bolt-bonded > bolted > bonded order. No peeling effect or plastic deformation was observed on the glued surfaces in the tensile samples in all groups. It was seen that the bolt holes were deformed along the loading direction in bolted and bolted bonded samples and fiber extraction and delamination occurred around the hole in carbon fiber samples.

- According to the four-point bending test, force-displacement values of the AZ91-AZ91, AZ91-CF, CF-CF bonded, bolted and bolted-bonded-single lap plate joints, the maximum shear force value was determined in ~1600 N in CF-CF bolted-bonded samples and the highest maximum displacement value was approximately ~18 mm in CF-CF bolted-bonded samples. The adhesive failure was dominant for the adhesive-sticky pairs in all groups. The absence of peeling in the separated samples (Figure 12d,g) indicates that there is good adhesion at the adhesive and material interface.
- As a result, it is thought that the bolted-bonded single lap plate joints produced by the AZ91 Mg alloy and carbon fiber plate by using Acryton 1E1 adhesive among themselves and with each other can be used in line with the data obtained in applications that require light weight, structural strength, and bonding with different methods.

Author Contributions: Conceptualization, F.K. and A.S.; methodology, F.K. and A.S.; investigation, A.S. and F.K.; Writing—review & editing, F.K. and A.S. All authors have read and agreed to the published version of the manuscript.

Funding: This study was supported by the Gümüşhane University Scientific Research Projects Coordinatorship (GÜBAP, Project Number: 23.E0117.07.01).

Conflicts of Interest: The authors declare no conflict of interest.

References

1. Keller, T.; Vallée, T. Adhesively bonded lap joints from pultruded GFRP profiles. Part I: Stress–strain analysis and failure modes. *Compos. Part B Eng.* **2005**, *36*, 331–340.
2. Niklaus, F.; Stemme, G.; Lu, J.Q.; Gutmann, R.J. Adhesive wafer bonding. *J. Appl. Phys.* **2006**, *99*, 031101.
3. Brockmann, W.; Geiß, P.L.; Klingens, J.; Schröder, K.B. *Adhesive Bonding: Materials, Applications and Technology*; John Wiley & Sons: Hoboken, NJ, USA, 2008.
4. Ebnesajjad, S. Characteristics of adhesive materials. In *Handbook of Adhesives and Surface Preparation*; William Andrew Publishing: Norwich, NY, USA, 2011; pp. 137–183.
5. Ebnesajjad, S.; Landrock, A.H. *Adhesives Technology Handbook*; William Andrew: Norwich, NY, USA, 2014.
6. Stagon, S.; Knapp, A.; Elliott, P.; Huang, H. Metallic glue for ambient environments making strides: Advancements in nanoscience are making it possible to metallurgically glue two solids together at room temperature, in air, and under a small amount of mechanical pressure. *Adv. Mater. Process.* **2016**, *1*, 22–26.
7. Goh, G.D.; Yap, Y.L.; Agarwala, S.; Yeong, W.Y. Recent progress in additive manufacturing of fiber reinforced polymer composite. *Adv. Mater. Technol.* **2019**, *4*, 1800271.
8. Petrie, E.M. *Handbook of Adhesives and Sealants*; McGraw-Hill Education: Chicago, IL, USA, 2007.
9. Da Silva, L.F.; Pironi, A.; Öchsner, A. *Hybrid Adhesive Joints*; Springer Science + Business Media: Berlin/Heidelberg, Germany, 2011; Volume 6.
10. Mouritz, A.P. *Introduction to Aerospace Materials*; Elsevier: Amsterdam, The Netherlands, 2012.
11. García-Moreno, F. Commercial applications of metal foams: Their properties and production. *Materials* **2016**, *9*, 85.
12. Meschut, G.; Merklein, M.; Brosius, A.; Drummer, D.; Fratini, L.; Füssel, U.; Gude, M.; Homberg, W.; Martins, P.A.F.; Bobbert, M.; et al. Review on mechanical joining by plastic deformation. *J. Adv. Join. Process.* **2022**, *5*, 100113.
13. Higgins, A. Adhesive bonding of aircraft structures. *Int. J. Adhes. Adhes.* **2000**, *20*, 367–376.
14. Banea, M.D.; da Silva, L.F. The effect of temperature on the mechanical properties of adhesives for the automotive industry. *Proc. Inst. Mech. Eng. Part L J. Mater. Des. Appl.* **2010**, *224*, 51–62.
15. Jeevi, G.; Nayak, S.K.; Abdul Kader, M. Review on adhesive joints and their application in hybrid composite structures. *J. Adhes. Sci. Technol.* **2019**, *33*, 1497–1520.
16. Zhou, A.; Keller, T. Joining techniques for fiber reinforced polymer composite bridge deck systems. *Compos. Struct.* **2005**, *69*, 336–345.
17. Silva, M.R.G.; Marques, E.A.S.; Silva, L. Behaviour under impact of mixed adhesive joints for the automotive industry. *Lat. Am. J. Solids Struct.* **2016**, *13*, 835–853.
18. Kožuh, Z.; Kralj, S.; Cvirin, Ž. Advantages and application possibilities of adhesive bonding. *Promet-Traffic Transp.* **1997**, *9*, 33–40.

19. Adderley, C.S. Adhesive bonding. *Mater. Des.* **1988**, *9*, 287–293.
20. Loureiro, A.L.; Da Silva, L.F.; Sato, C.; Figueiredo, M.A.V. Comparison of the mechanical behaviour between stiff and flexible adhesive joints for the automotive industry. *J. Adhes.* **2010**, *86*, 765–787.
21. Adams, R.D. *Adhesive Bonding: Science, Technology and Applications*; Woodhead Publishing: Cambridge, UK, 2021.
22. Adams, R.D.; Comyn, J.; Wake, W.C. *Structural Adhesive Joints in Engineering*; Springer Science & Business Media: Berlin/Heidelberg, Germany, 1997.
23. Banea, M.D.; da Silva, L.F. Adhesively bonded joints in composite materials: An overview. *Proc. Inst. Mech. Eng. Part L J. Mater. Des. Appl.* **2009**, *223*, 1–18.
24. Barnes, T.A.; Pashby, I.R. Joining techniques for aluminium spaceframes used in automobiles: Part II—Adhesive bonding and mechanical fasteners. *J. Mater. Process. Technol.* **2000**, *99*, 72–79.
25. Czerwinski, F. *Magnesium Alloys: Design, Processing and Properties*; BoD—Books on Demand: Norderstedt, Germany, 2011.
26. Baldan, A. Adhesion phenomena in bonded joints. *Int. J. Adhes. Adhes.* **2012**, *38*, 95–116.
27. Prasad, S.S.; Prasad, S.B.; Verma, K.; Mishra, R.K.; Kumar, V.; Singh, S. The role and significance of Magnesium in modern day research—A review. *J. Magnes. Alloys* **2022**, *10*, 1–61.
28. Aghion, E.; Bronfin, B.; Eliezer, D. The role of the magnesium industry in protecting the environment. *J. Mater. Process. Technol.* **2001**, *117*, 381–385.
29. Hirsch, J.; Al-Samman, T. Superior light metals by texture engineering: Optimized aluminum and magnesium alloys for automotive applications. *Acta Mater.* **2013**, *61*, 818–843.
30. Karaguiozova, Z.; Miteva, A.; Ciski, A.; Cieslak, G. Magnesium Application in Aerospace Industry. In Proceedings of the 12th Scientific Conference Space Ecology Safety, Sofia, Bulgaria, 2–4 November 2016; pp. 2–4.
31. Luo, A.; Pekguleryuz, M.O. Cast magnesium alloys for elevated temperature applications. *J. Mater. Sci.* **1994**, *29*, 5259–5271. [[CrossRef](#)]
32. Baghni, I.M.; Wu, Y.S.; Li, J.Q.; Du, C.W.; Zhang, W. Mechanical properties and potential applications of magnesium alloys. *Trans. Nonferrous Met. Soc. China-Engl. Ed.* **2003**, *13*, 1253–1259.
33. Wang, G.G.; Weiler, J.P. Recent developments in high-pressure die-cast magnesium alloys for automotive and future applications. *J. Magnes. Alloys* **2022**, *11*, 78–87. [[CrossRef](#)]
34. Hisao, W. Trend of Research and Development for Magnesium Alloys. *Sci. Technol. Trends Q. Rev.* **2006**, *18*, 84–97.
35. Aghion, E.; Bronfin, B. Magnesium alloys development towards the 21st century. In *Materials Science Forum*; Trans Tech Publications Ltd.: Zurich, Switzerland, 2000; Volume 350, pp. 19–30.
36. Liu, B.; Yang, J.; Zhang, X.; Yang, Q.; Zhang, J.; Li, X. Development and application of magnesium alloy parts for automotive OEMs: A review. *J. Magnes. Alloys* **2023**, *11*, 15–47. [[CrossRef](#)]
37. Kelly, G. Load transfer in hybrid (bonded/bolted) composite single-lap joints. *Compos. Struct.* **2005**, *69*, 35–43. [[CrossRef](#)]
38. Colombi, P.; Poggi, C. Strengthening of tensile steel members and bolted joints using adhesively bonded CFRP plates. *Constr. Build. Mater.* **2006**, *20*, 22–33. [[CrossRef](#)]
39. Reis, P.N.; Ferreira, J.A.M.; Antunes, F. Effect of adherend’s rigidity on the shear strength of single lap adhesive joints. *Int. J. Adhes. Adhes.* **2011**, *31*, 193–201. [[CrossRef](#)]
40. Sayman, O. Elasto-plastic stress analysis in an adhesively bonded single-lap joint. *Compos. Part B Eng.* **2012**, *43*, 204–209. [[CrossRef](#)]
41. Liao, L.; Huang, C.; Sawa, T. Effect of adhesive thickness, adhesive type and scarf angle on the mechanical properties of scarf adhesive joints. *Int. J. Solids Struct.* **2013**, *50*, 4333–4340. [[CrossRef](#)]
42. Rahman, N.M.; Sun, C.T. Strength calculation of composite single lap joints with Fiber-Tear-Failure. *Compos. Part B Eng.* **2014**, *62*, 249–255. [[CrossRef](#)]
43. Selahi, E. Failure study of hybrid bonded-bolted composite single and double lap joints. *J. Stress Anal* **2019**, *3*, 37–46.
44. Silva, T.C.; Nunes, L.C.S. A new experimental approach for the estimation of bending moments in adhesively bonded single lap joints. *Int. J. Adhes. Adhes.* **2014**, *54*, 13–20. [[CrossRef](#)]
45. Li, X.; Tan, Z.; Wang, L.; Zhang, J.; Xiao, Z.; Luo, H. Experimental investigations of bolted, adhesively bonded and hybrid bolted/bonded single-lap joints in composite laminates. *Mater. Today Commun.* **2020**, *24*, 101244. [[CrossRef](#)]
46. Ye, J.; Yan, Y.; Li, J.; Hong, Y.; Tian, Z. 3D explicit finite element analysis of tensile failure behavior in adhesive-bonded composite single-lap joints. *Compos. Struct.* **2018**, *201*, 261–275. [[CrossRef](#)]
47. Belardi, V.G.; Fanelli, P.; Vivio, F. Analysis of multi-bolt composite joints with a user-defined finite element for the evaluation of load distribution and secondary bending. *Compos. Part B Eng.* **2021**, *227*, 109378. [[CrossRef](#)]
48. Chen, Y.; Yang, X.; Li, M.; Wei, K.; Li, S. Mechanical behavior and progressive failure analysis of riveted, bonded and hybrid joints with CFRP-aluminum dissimilar materials. *Thin-Walled Struct.* **2019**, *139*, 271–280. [[CrossRef](#)]
49. Hirsch, J. Recent development in aluminium for automotive applications. *Trans. Nonferrous Met. Soc. China* **2014**, *24*, 1995–2002. [[CrossRef](#)]
50. *ASTM D3165-07*; Standard Test Method for Strength Properties of Adhesives in Shear by Tension Loading of Single-Lap-Joint Laminated Assemblies. Annual Book of ASTM Standard: West Conshohocken, PA, USA, 2014; Volume 6, p. 15.
51. *ASTM 3039*; ASTM Committee D-30 on Composite Materials. Standard Test Method for Tensile Properties of Polymer Matrix Composite Materials. ASTM International: West Conshohocken, PA, USA, 2008.

52. ASTM D1002; Standard Test Method for Apparent Shear Strength of Single-Lap-Joint Adhesively Bonded Metal Specimens by Tension Loading (Metal-to-Metal). ASTM International: West Conshohocken, PA, USA, 2005; Volume 15, pp. 45–48.
53. Karabudak, F. High-cycle fatigue and tensile strength of AZ91 Mg alloy with MAO-epoxy duplex coating. *Met. Mater. Kov. Mater.* **2023**, *61*, 81–90. [[CrossRef](#)]
54. Kandil, A. Microstructure and mechanical properties of SiCp/AZ91 magnesium matrix composites processed by stir casting. *JES J. Eng. Sci.* **2012**, *40*, 255–270. [[CrossRef](#)]
55. Luo, H.; Tan, Y.; Zhang, F.; Zhang, J.; Tu, Y.; Cui, K. Selectively enhanced 3D printing process and performance analysis of continuous carbon fiber composite material. *Materials* **2019**, *12*, 3529. [[CrossRef](#)]
56. Motavallian, P.; Rabiee, S.M.; Aval, H.J. Effect of solution treatment of AZ91 alloy on microstructure, mechanical properties and corrosion behavior of friction stir back extruded AZ91/bioactive glass composite. *J. Mater. Res. Technol.* **2023**, *25*, 6992–7007. [[CrossRef](#)]
57. Li, H.; Liebscher, M.; Zhao, D.; Yin, B.; Du, Y.; Yang, J.; Mechtcherine, V. A review of carbon fiber surface modification methods for tailor-made bond behavior with cementitious matrices. *Prog. Mater. Sci.* **2022**, *132*, 101040. [[CrossRef](#)]
58. Lu, M.; Xiao, H.; Liu, M.; Feng, J. Carbon fiber surface Nano-modification and enhanced mechanical properties of fiber reinforced cementitious composites. *Constr. Build. Mater.* **2023**, *370*, 130701. [[CrossRef](#)]

Disclaimer/Publisher’s Note: The statements, opinions and data contained in all publications are solely those of the individual author(s) and contributor(s) and not of MDPI and/or the editor(s). MDPI and/or the editor(s) disclaim responsibility for any injury to people or property resulting from any ideas, methods, instructions or products referred to in the content.